CHEMISTRY
A EUROPEAN JOURNAL

DOI: 10.1002/chem.201000783

The Intramolecular Interaction of Thiophene and Furan with Aromatic and Fluoroaromatic Systems in Some [3.3]Meta(heterocyclo)paracyclophanes: A Combined Computational and NMR Spectroscopic Study

Maurizio Benaglia,[a] Franco Cozzi,*[a] Michele Mancinelli,[b] and Andrea Mazzanti*[b]

Dedicated to Professor Lodovico Lunazzi on the occasion of his 70th birthday

Abstract: Four thiophene- and furan-containing [3.3]meta(heterocyclo)paracyclophanes were designed and synthesized to study the intramolecular interaction between standard heteroaromatic rings and tetra-H- or tetra-F-substituted benzenes. A complete conformational analysis, carried out by DFT calculations and variable-temperature NMR techniques, showed that, despite their structural similarity, these adducts have different conformational preferences and undergo different types of isomerizations depending on the nature of the heterocycle. The thiophene-derived adducts adopted a parallel stacked arrangement of the aromatic systems in the ground-state conformations. Their isomerization pathways involved a thiophene ring-flip process passing through an edge-to-face arranged transition state in which the heterocycle is perpendicular to the benzene platform and its sulfur atom points toward the center of that ring. The threshold energy barrier to the ring-flip process was higher by 10 kJ mol^{-1} in the case of the adduct featuring the perfluorinated benzene. This difference was rationalized by assuming that the ground-state conformations of the H- and F-substituted compounds have different stability. On the contrary, the furan-derived adducts were shown by calculations and NMR spectroscopy to adopt, in their ground-state conformations, a perpendicular edge-to-face disposition of the rings with the oxygen atom pointing toward the benzene platform. The adoption of this arrangement was confirmed by X-ray crystallography. In the case of these compounds, the isomerization process involved distortion of the CH_2SCH_2 bridges connecting the aromatic systems and the adoption of transition-state geometries for which the rings were arranged in a parallel-stacked orientation. Once again a very nice agreement was observed between the predicted and the experimentally determined geometries and pathways. In the case of the furan-containing compounds, the threshold barriers were found to be much lower in energy that those observed for the thiophene derivatives. Remarkably, they were virtually independent of the presence of fluorine atoms on the platform benzene ring.

Keywords: arene–arene interactions · conformational analysis · fluoroaromatic compounds · NMR spectroscopy · pi interactions

Introduction

Arene–arene interactions[1] have been shown to play a central role in determining the structures of supramolecular adducts,[2] organic crystals,[3] and macrobiomolecules.[4] They also mediate several molecular recognition events in biological systems.[5] Whereas the wide majority of the theoretical and experimental works have studied the arene–arene interactions occurring between standard aromatic systems (typically, benzene and substituted benzenes),[1,6] only a surprisingly limited number of investigations have been devoted to elucidate the interactions between simple arenes and paradigmatic heteroarenes,[7] such as pyridine,[7a,d,e,g,h,i)] furan,[7b] and thiophene.[7b,c,d,f] This is even more amazing when one

[a] Prof. M. Benaglia, Prof. F. Cozzi
Dipartimento di Chimica Organica e Industriale
Università degli Studi di Milano
Via Golgi 19, 20133, Milano (Italy)
Fax: (+39) 02-50314159
E-mail: franco.cozzi@unimi.it

[b] Dr. M. Mancinelli, Dr. A. Mazzanti
Dipartimento di Chimica Organica "A.Mangini"
Università degli Studi di Bologna
Viale Risorgimento 4, 40136 Bologna (Italy)
Fax: (+39) 051-2093633
E-mail: mazzand@ms.fci.unibo.it

Supporting information for this article is available on the WWW under http://dx.doi.org/10.1002/chem.201000783.

WILEY InterScience DISCOVER SOMETHING GREAT
© 2010 Wiley-VCH Verlag GmbH & Co. KGaA, Weinheim

considers that such a study could help us to understand not only how the presence of the heteroatom affects the interaction between the π systems, but also how the heteroatom itself can interact with the π electrons of the arene. The latter aspect is particularly relevant since it can contribute to the investigation of lone-pair-π and anion-π interactions, a new type of nonbonding interactions that are receiving increasing attention to help design and explain chemical and biochemical molecular recognition events.[8]

As a part of our continuing interest in developing model systems to study arene–arene interactions,[9] we have recently reported a combined computational and NMR spectroscopic study on the intramolecular interaction between pyridine and aromatic and fluoroaromatic systems in 2,11-dithia[3.3](2,6)pyridinoparacyclophanes **1** and **2** (Figure 1).[10]

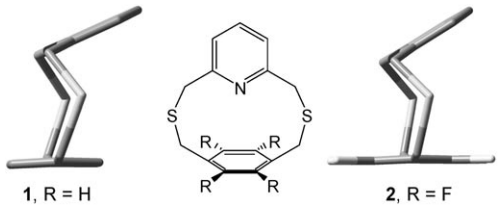

Figure 1. Structure of [3.3](2,6)pyridinoparacyclophanes **1** and **2**, and side views of their ground-state conformations showing a tilted edge-to-face disposition of the aromatic rings.

It was shown that, in their most stable conformation, these molecules adopt a tilted edge-to-face (EtF) disposition of C_s symmetry, with the N-atom pointing toward the face of the benzene ring. Both adducts topomerize by a facile flip of the heterocyclic ring, a process that is required to overcome a barrier of only 22.6 and 26.6 kJ mol^{-1} for **1** and **2**, respectively, as experimentally determined by variable-temperature (VT) NMR spectroscopy. For both **1** and **2**, a C_2 orthogonal EtF conformation is encountered along the ring-flip pathway, in which the nitrogen lone pair points toward the center of the platform benzene ring. Interestingly, this conformation was shown to be a low-energy transition state for adduct **1** and a high-energy minimum for adduct **2**, which indicates in the latter a favorable interaction between the nitrogen lone pair and the tetrafluoro-substituted arene system.

These results suggested that 2,11-dithia[3.3]-metaparacyclophanes like **1** and **2** can provide readily accessible model systems to study the arene–heteroarene interaction for which the interacting π systems can adopt different relative orientations. Therefore, we decided to extend the study carried out on **1** and **2** to related systems for which penta-atomic heteroaromatic rings, such as thiophene and furan replace pyridine. Here, we wish to report the results of this study.

Results

Synthesis: 2,11-Dithia[3.3]metaparacyclophanes **3–6** were obtained as described in Scheme 1. Reaction of 2,5-bisbromomethylthiophene **7**[11] with commercially available 1,4-bis(mercaptomethyl)benzene under high-dilution conditions[7c] afforded adduct **3** in 18% yield. The corresponding furan derivative **5** could not be obtained by the same procedure, likely because of the high instability of 2,5-bisbromomethylfuran **8**.[12] To circumvent this problem, compound **8** was converted into 2,5-bismercaptomethylfuran **10** by following a literature procedure,[13a] and was then reacted with commercially available 1,4-bisbromomethylbenzene to afford adduct **5** in 20% yield. The tetrafluoro-substituted cyclophanes **4** and **6** were likewise obtained by reaction of the heterocyclic 2,5-bis(mercaptomethyl) derivatives **9**[13b] and **10** with 1,4-bisbromomethyl-2,3,5,6-tetrafluoro-benzene[14] (22 and 10% yield for **4** and **6**, respectively).

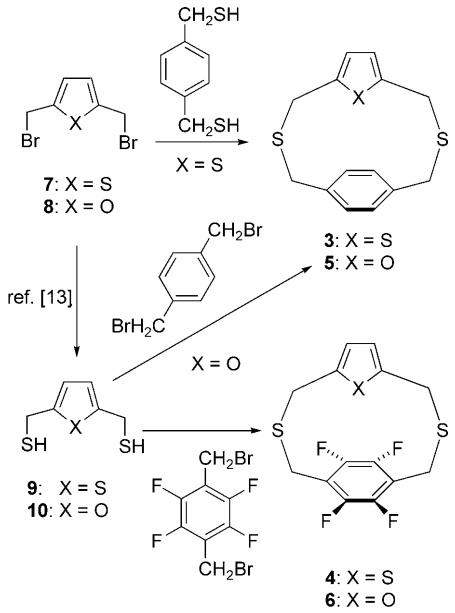

Scheme 1. Synthesis of cyclophanes **3–6**.

Computational and VT-NMR spectroscopic studies of thiophene-containing adducts 3 and 4: There is a major geometric difference between pyridine-derived compounds **1** and **2** on one side and thiophene- or furan-containing adducts **3–6** on the other. As pointed out several years ago by Vögtle and Lichtentäler for 2,10-dithia[3.3](2,5)thiophenophane,[15] the angle between the bonds exiting from the positions adjacent to the heteroatom changes markedly on passing from hexa-atomic pyridine (120°) to penta-atomic thiophene (147°). A wider angle implies a shorter distance between the aromatic rings in compounds **3** and **4** than that observed in **1** and **2**.

To localize all the energy minima for adducts **3** and **4**, a preliminary conformational search by molecular mechanics

 © 2010 Wiley-VCH Verlag GmbH & Co. KGaA, Weinheim

(MM) methods was performed. All the energy minima found within a 20 kJ mol^{-1} window from the global minimum were then minimized with DFT at the B3LYP/6-311++G(2d,p) level of theory.[16] In the case of adduct **4**, DFT minimization clustered the solutions of the MM search around the three ground states (GS) shown in Figure 2.

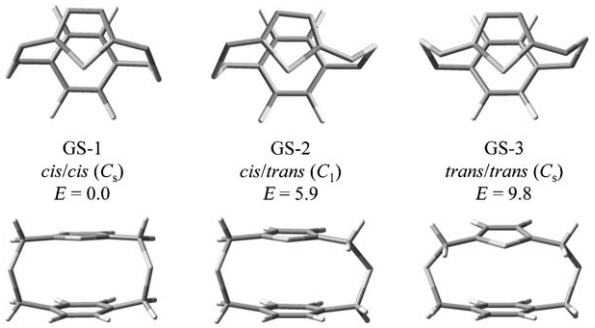

Figure 2. Top and front views of the three ground state conformations calculated for adduct **4**. Energies in kJ mol^{-1}.

These conformations differ for the relative disposition of the sulfur atoms of the CH_2SCH_2 bridges with respect to that of the heterocycle. Thus, the C_s conformation for which these sulfur atoms point toward the same direction is defined as *cis*/*cis*. This is calculated to be the most stable (GS-1). The second best conformation GS-2 (+5.9 kJ mol^{-1}) shows a *cis*/*trans* arrangement and exhibits C_1 symmetry. The highest energy conformation GS-3 (+9.8 kJ mol^{-1}) has C_s symmetry and a *trans*/*trans* disposition. All of these structures show a virtually parallel-stacked (PS) arrangement of the two rings, the interplanar angles being −7, ≈ 0, and 9° for GS-1, GS-2, and GS-3, respectively.[17] The energy difference between GS-1 and GS-2, should allow also for the population of the latter conformation to be detected by NMR spectroscopy when the thiophene ring-flip movement is frozen. On the contrary, the GS-3 conformation seems to be too high in energy to be significantly populated.

The stereodynamic pathway of the thiophene ring flip above the benzene platform was analyzed by means of DFT calculations at the B3LYP/6-311++G(2d,p) level (Figure 3). By starting from the *cis*/*cis* GS-1 conformation a first transition state (TS-1) exchanges the orientation of one of the bridges and leads to *cis*/*trans* GS-2. From this geometry, the thiophene ring can flip over the *para*-substituted benzene ring adopting a T-shaped, C_2-symmetric, high-energy transition structure (TS-2) in which the heterocyclic ring is orthogonal to the plane of the aromatic ring. This TS represents the halfway point of the whole process, from which the topomerization pathway is completed by visiting enantiomeric GS-2′ and TS-1′ conformations. The geometries of the TS were verified by frequency analysis at the same level of theory (i.e. B3LYP/6-311++G(2d,p)), which showed that a single imaginary frequency was present, and that the corresponding normal mode was indeed related to the motion of one the sulfur bridge (TS-1) or to the flip of

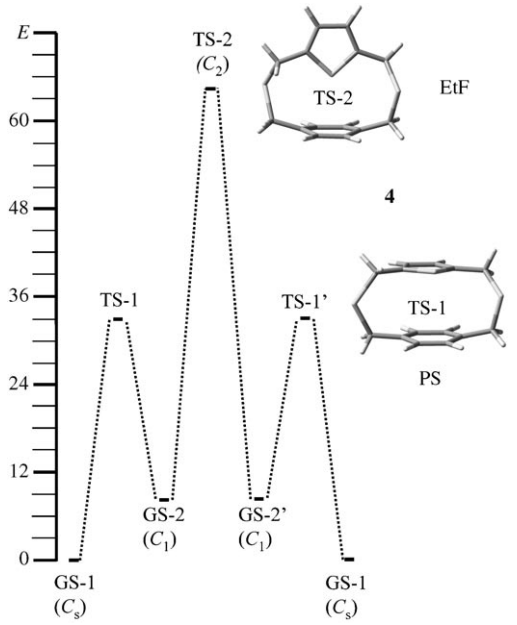

Figure 3. B3LYP/6-311++G(2d,p) calculated pathways and energy profile for the topomerization of thiophene-containing cyclophane **4**. Energies in kJ mol^{-1}.

thiophene (TS-2). The two TS were 31.4 and 58.6 kJ mol^{-1} higher in energy than the global minimum GS-1. Therefore, the threshold conformation for the thiophene ring-flip process corresponds to TS-2.

The calculations predicted that the same stereodynamic pathway is followed in the case of cyclophane **3**. Also for this compound, DFT calculations showed that the *cis*/*cis* conformation is the most stable one (GS-1), and the *cis*/*trans* one is the second best (GS-2). In this case, however, the energy difference is smaller (only 1.2 kJ mol^{-1}, Table 1),

Table 1. B3LYP/6-311++G(2d,p) calculated and experimental energies (in kJ mol^{-1}) for different conformations of thiophene-containing cyclophanes **3** and **4**.

	Ground-state energies			TS energies		Exptl. values	
	cis/*cis*	*cis*/*trans*	*trans*/*trans*	C_2	C_1	TS-2	TS-1
	GS-1	GS-2	GS-3	TS-2	TS-1		
3 (H)	0.0	1.2	2.8	49.4	32.6	46.9	35.1
4 (F)	0.0	5.9	9.8	58.6	31.4	56.9	36.0

and a larger population for the GS-2 conformer is expected. The calculated TS-1 and TS-2 energies correspond to 32.6 and 49.4 kJ mol^{-1} for the CH_2SCH_2 bridge interconversion and for the thiophene ring-flip processes, respectively (see Table 1). While postponing any comment to the Discussion section, it must be noted here that the fluorinated cyclophane **4** is predicted to have a strikingly higher topomerization threshold barrier than hydrogen-substituted adduct **3**.

In principle, if the energy barriers predicted by the calculations for adduct **4** were correct, both processes (bridge isomerization and ring-flip movement) should be observable by

 © 2010 Wiley-VCH Verlag GmbH & Co. KGaA, Weinheim

dynamic NMR spectroscopy. If only the population of the *cis*/*cis* GS-1 structure were detectable, the ^{1}H NMR spectrum of this conformation would show anisochronous signals for the diastereotopic methylene groups of the bridges, which are not related by the molecular plane of symmetry,[18] and two AB systems should be observed when the ring-flip motion is frozen. On the other hand, if both the *cis*/*cis* GS-1 and *cis*/*trans* GS-2 conformations were sufficiently populated, they can be distinguished because the GS-2 conformation, being asymmetric (C_1), would show complex NMR spectra comprising four AB systems for the methylene groups and two coupled thiophene hydrogen atoms in the ^{1}H-, and two pairs of *ortho*-coupled fluorine atoms in the ^{19}F NMR spectra, respectively.

The 600 MHz ^{1}H NMR spectrum of compound **4** recorded at room temperature in CD_2Cl_2 showed two broad signals for the two constitutionally heterotopic methylenes of the CH_2SCH_2 bridges. These signals broadened further on lowering the temperature, and eventually split into two AB systems below 0 °C (J_{AB} = 15.7 and 14.8 Hz; Figure 4). By line shape simulation, an activation energy of 56.9 kJ mol^{-1} was derived, in good agreement with the calculated value (58.6 kJ mol^{-1}). By the same temperature variation, the ^{19}F NMR (564.6 MHz, CD_2Cl_2) signal corresponding to the four fluorine atoms of the *para*-substituted benzene ring observed at room temperature split into two somewhat broad signals in a 1:1 ratio (thus, each signal accounts for two fluorine atoms), as the consequence of a partial loss of symmetry of the aromatic ring.

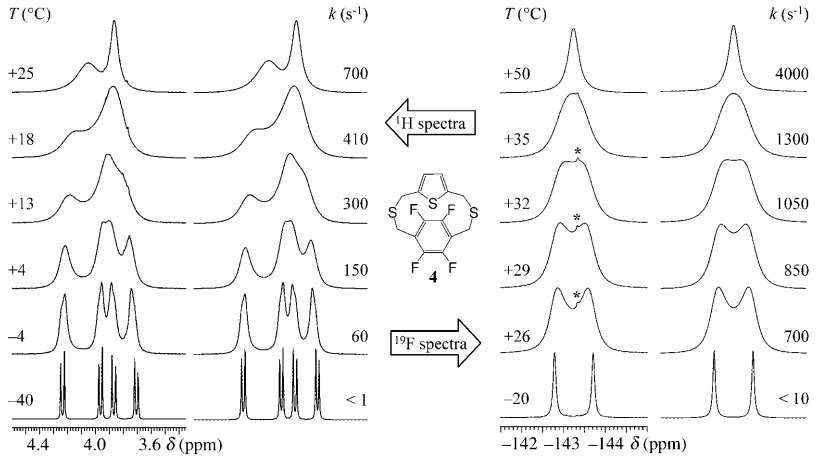

Figure 4. VT-NMR spectra of adduct **4**: Left: ^{1}H NMR spectra (600 MHz in CD_2Cl_2) of compound **4**, together with the line shape simulation and rate constants. Right: ^{19}F NMR spectra (564.6 MHz in $CDCl_3$) with the corresponding simulations. The asterisks in the ^{19}F spectra indicate an impurity.

It should be noted that the two signals are not coupled, which indicates that below −20 °C the two sides of the phenyl are no longer dynamically symmetry equivalent, while the molecule still features a plane of symmetry.[19] The energy barrier derived by the line shape simulation of the ^{19}F NMR spectra was identical to that observed in the proton spectra (56.9 kJ mol^{-1}). The observed lack of symmetry of the fluorinated benzene ring implies that the ring flip of thiophene is frozen, and the rotation of the fluorinated ring is also blocked. The identical values determined by ^{1}H- and ^{19}F NMR spectroscopy suggest that the barrier to benzene rotation is higher than that to the thiophene ring flip, but it cannot be observed unless the lower-energy motion is also frozen.[20] On the basis of the calculations and of the large energy difference between C_s-symmetric GS-1 and GS-3 (see above), it is reasonable to assign the GS-1 structure to the only $\boldsymbol{C_s}$ conformation observed at low temperature for cyclophane **4**.

The NMR spectra of adduct **4** were then recorded at a lower temperature in the attempt to determine experimentally also the energy barrier corresponding to the low-energy TS-2 (namely, the one corresponding to bridge interconversion). At −40 °C, both the ^{1}H- and ^{19}F NMR spectra (in $CDFCl_2$/CHF_2Cl) showed that the isomerization due to the movement of the bridges was still rapid or that only one conformation was populated. However, on a further lowering of the temperature, the ^{19}F spectra showed that the two signals still observed at −40 °C broadened around −90 °C and became sharp again below −100 °C. This is the typical behavior of an exchange between two conformations with very different population.[21] On further lowering the temperature to −128 °C, four additional ^{19}F signals appeared, with very different chemical shifts, but with identical relative intensity (indicated by the arrows in Figure 5, bottom trace). These signals reversibly disappeared and appeared again on raising and lowering the temperature and they should be assigned to a second conformation. The presence of four F signals is compatible only with the C_1-symmetric *cis*/*trans* conformation GS-2, the second-best GS predicted by the calculations for cyclophane **4**.

By careful integration of the ^{19}F NMR spectrum recorded at −128 °C, a 0.5–0.7 % population was determined for the minor conformation, corresponding to an experimental energy difference between GS-1 and GS-2 of ΔG° = 6.3 kJ mol^{-1}, in very good agreement with the calculated value of 5.9 kJ mol^{-1}. From the line shape simulation of the ^{19}F NMR spectra of adduct **4**, a barrier of 36.0 kJ mol^{-1} was derived, in line with that predicted by DFT calculations (31.4 kJ mol^{-1}).

VT-^{1}H NMR spectroscopic analysis carried out on thiophene-derived cyclophane **3** showed that this adduct behaved very similarly to its fluorinated counterpart **4**. In par-

 © 2010 Wiley-VCH Verlag GmbH & Co. KGaA, Weinheim

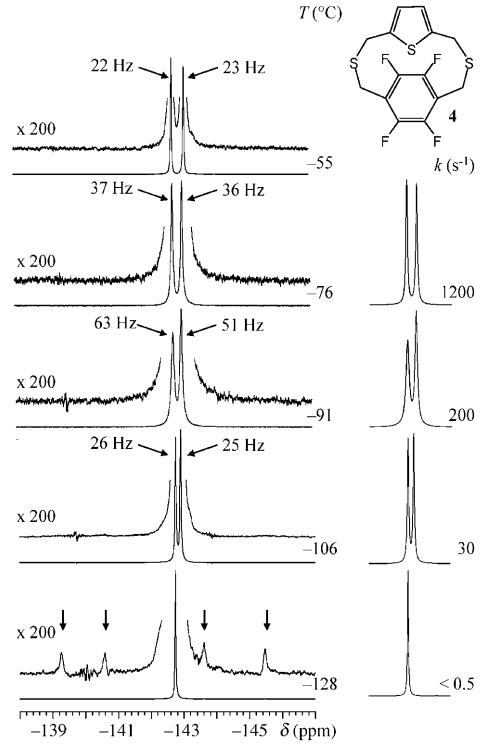

Figure 5. Left: ^{19}F NMR spectra of compound **4** (564.6 MHz in $CDFCl_2$/CHF_2Cl). The signals belonging to the C_1 conformation are indicated with the arrows in the spectrum at −128 °C. Right: line shape simulation with the corresponding rate constants. (Note: the major signals get closer on lowering the temperature, and eventually overlap at −128 °C).

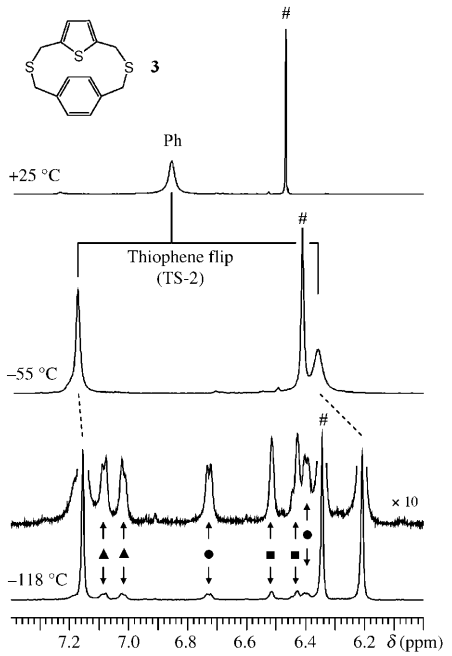

Figure 6. Aromatic region of the ^{1}H spectrum of **3** (600 MHz in CD_2Cl_2/$CBrF_3$ 10:1 v/v). The spectrum at −118 °C shows the presence and multiplicity of the minor conformer (22% population). Signals marked with ▲ and ● belong to the four phenyl protons, whereas ■ indicates the signals belonging to the thiophene protons. # indicates the thiophene hydrogen atoms signal of the major conformation.

ticular, a threshold barrier for the thiophene ring-flip process of 46.9 kJ mol^{-1} and a lower-energy barrier for the bridge isomerization of 35.1 kJ mol^{-1} were determined for **3** (see Table 1 and Figure 6).

Both these values are in good agreement with those predicted by the calculations (49.4 and 32.6 kJ mol^{-1}, respectively). Also the population of 22% for the second best GS conformation (GS-2), experimentally determined by integration of the signals at −118 °C (see Figure 6), nicely agrees with the 28% one calculated (at −118 °C) on the basis of the computed difference in stability between GS-1 and GS-2 ($\Delta E = 1.2$ kJ mol^{-1}).

Computational and VT-NMR spectroscopic studies of furan-containing adducts 5 and 6: The replacement of the thiophene ring of cyclophanes **3** and **4** with the furan ring of compounds **5** and **6** exerts a dramatic effect on the conformational preferences of these compounds. Indeed, DFT computations, carried out after the preliminary MM search (see above) in the case of adduct **6**, predicted as the lowest-energy conformation the one indicated as GS-4 in Figure 7.

This conformation features an orthogonal EtF disposition of the aromatic rings, with the furan oxygen pointing toward the centroid of the aromatic ring. Because of the *trans* disposition of the CH_2SCH_2 bridges, GS-4 has C_2 symmetry. In addition, three other conformations were identified as energy minima for compound **6**, namely, the tilted EtF GS-3

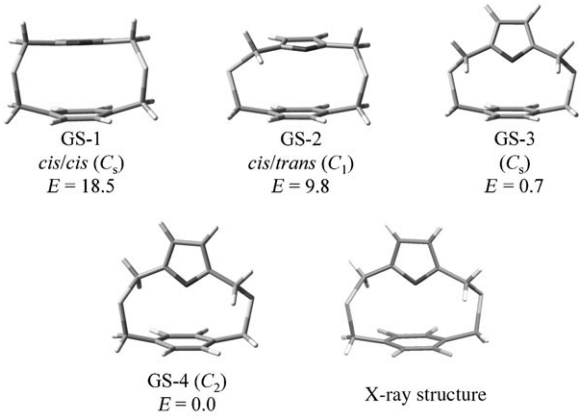

Figure 7. Front views of the four ground-state conformations calculated for adduct **6** and X-ray structure. Energies in kJ mol^{-1}.

(C_s symmetry, +0.7 kJ mol^{-1}), the PS *cis*/*trans* GS-2 (C_1 symmetry, +9.8 kJ mol^{-1}), and the PS *cis*/*cis* GS-1 (C_s symmetry, +18.5 kJ mol^{-1}). While both GS-1 and GS-2 are closely related to the corresponding structures calculated for the thiophene-containing adduct **4**, it is worth mentioning that GS-3 of adduct **6** features a much wider interplanar angle (66°) than GS-3 of **4** (9°) and it is only marginally less stable than GS-4.

To our delight, X-rays analysis of a crystal of adduct **6** confirmed the structure calculated as the global minimum for adduct **6**. The determination of this structure is relevant

 © 2010 Wiley-VCH Verlag GmbH & Co. KGaA, Weinheim

in general and for this work in particular. In general because, to the best of our knowledge, this is the first report of an experimental structure showing an orthogonal EtF arrangement of two aromatic systems in which a heteroatom on one ring points at short distance (2.90 Å) toward the centroid of another aromatic system (for further comments see below in the Discussion section). In particular, because the coincidence between the calculated and the experimentally determined structure suggests that the computational tool employed in this work is perfectly suitable to tackle the problem at hand.

The DFT computational analysis of adduct **5** (Table 2) identified the same four ground-state conformers found for adduct **6**. Their energies and geometries were similar to those predicted for compound **6** (Figure 8). In this case, however, the lowest-energy conformation was the tilted EtF disposition GS-3 with C_s symmetry (interplanar angle 36°), which was only 1.5 kJ mol^{-1} more stable than the C_2-symmetric, orthogonal EtF GS-4.

Table 2. B3LYP/6-311++G(2d,p) calculated and experimental energies (kJ mol^{-1}) for furan-containing cyclophanes **5** and **6**.

	Ground-state energies				TS energies		Exptl. values
	cis/*cis* GS-1	*cis*/*trans* GS-2	C_s GS-3	C_2 GS-4	TS-1	TS-2	TS-1
5 (H)	22.2	9.2	0.0	1.5	31.8	18.0[a]	29.7
6 (F)	18.4	9.8	0.7	0.0	33.0	19.2[a]	30.1

[a] Not detectable by NMR spectroscopy because of the negligible population of GS-2 (see text).

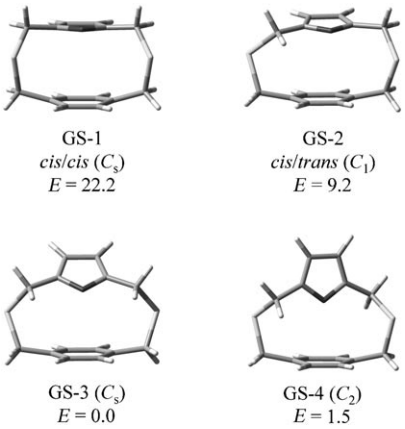

Figure 8. Front views of the four ground-state conformations calculated for adduct **5**. Energies in kJ mol^{-1}.

The isomerization pathway calculated for cyclophane **6** involves two transition states (Figure 9, left). By starting from the EtF disposition GS-4 (C_2), rotation of the bridges and flattening of the interplanar angle leads to PS GS-2 (C_1) passing through a transition state (TS-2) that is 18.0 kJ mol^{-1} higher in energy than GS-4. Since GS-2 is 9.8 kJ mol^{-1} higher in energy than GS-4, its population should not be detected by NMR spectroscopy (see below). Conformation GS-2 is then transformed into GS-3 of C_s symmetry passing through a second TS (TS-1), which is further higher in energy (+31.8 kJ mol^{-1}), and is reached through the movement of a CH_2SCH_2 bridge. This represents the threshold energy barrier for the interconversion of GS-4 into GS-3, a process that involves the inversion of the relative disposition of the two bridges. Remarkably, a TS for the direct isomerization of GS-4 into GS-3 (that is, an isomerization that does not require passing through GS-2) could not be located computationally. From these data it is evident that the threshold barrier for furan-derived adduct **6** is much lower than that observed for thiophene-derived adduct **4** (33.0 vs. 58.6 kJ mol^{-1}). This is not surprising, because the two interconversion processes involve different conformational movements: the thiophene ring flip in the case of adduct **4**; the sulfur bridge isomerization in the case of adduct **6**.

As in the case of adduct **6**, the calculated isomerization pathway of cyclophane **5** involves two transition states (Figure 9, right). By starting from the lowest-energy conformation, namely, the tilted EtF disposition GS-3 of C_s symmetry, the PS GS-2 conformation (+9.2 kJ mol^{-1}) is reached

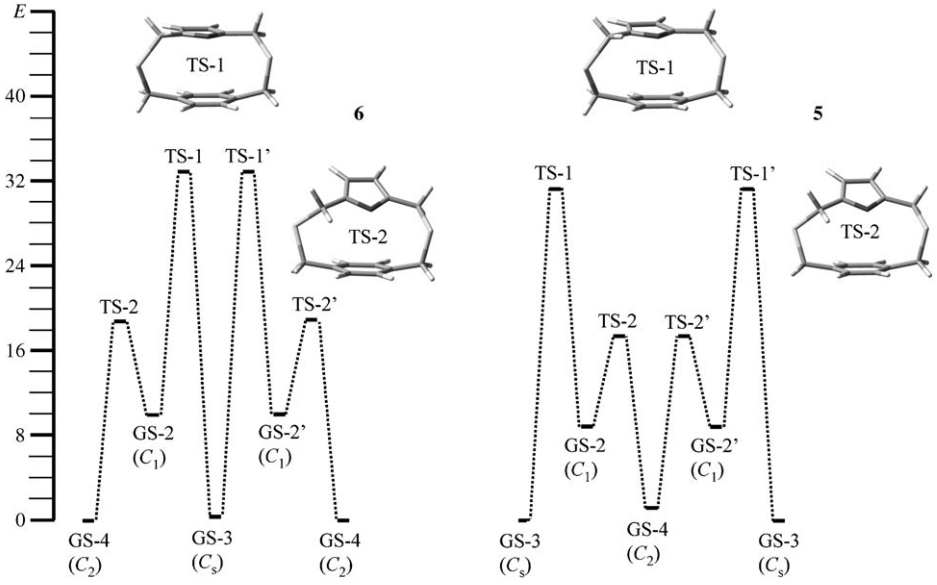

Figure 9. B3LYP/6-311++G(2d,p) calculated pathways and energy profiles for the topomerization of furan-containing cyclophanes **6** (left) and **5** (right). Energies in kJ mol^{-1}.

© 2010 Wiley-VCH Verlag GmbH & Co. KGaA, Weinheim

passing through a transition state (TS-1), which is 31.8 kJ mol^{-1} higher in energy. This process corresponds to the movement of one CH_2SCH_2 bridge, and represents the threshold barrier for this isomerization. As before, the GS-2 conformation should be too high in energy for its population to be detected by NMR spectroscopy (see below). Conformation GS-2 is then transformed into GS-4 of C_2 symmetry passing through a second transition state (TS-2), which is lower in energy (+18.0 kJ mol^{-1}). As in the case of adduct **6**, a TS for the direct isomerization of GS-3 into GS-4 could not be located, and the threshold barrier for furan-derived adduct **5** is much lower than that observed for its thiophene-derived counterpart **3** (+31.8 vs. +49.4 kJ mol^{-1}).

At a variance with adducts **3** and **4**, which have threshold TSs of clearly different energy, the two threshold TSs calculated of **5** and **6** are almost isoenergetic (31.8 and 33.0 kJ mol^{-1}, respectively). This is not unexpected because the threshold TSs correspond to the switch of one CH_2SCH_2 bridge, a process that should be only marginally influenced by the different substitution at the benzene platform in **5** and **6**.

The 564.6 MHz ^{19}F NMR spectrum of compound **6** recorded in $CDFCl_2/CBrF_3$ showed a single line down to −60 °C. On further lowering the temperature, the signal broadened and eventually split into two sets of two signals of different intensity and multiplicity at −138 °C (Figure 10, left). The two major signals were coupled with $^3J(F,F) = 21.0$ Hz, whereas the small signals were singlets (line width: 19 Hz). The coupled signals were necessarily assigned to two *ortho*-coupled, diastereotopic fluorine atoms on the same side of the benzene ring of the lowest-energy C_2-symmetric GS-4 conformation. Each of the small signals (6% population) belongs to two enantiotopic fluorine atoms on the same side of the benzene ring of the C_s-symmetric GS-3 conformation, the second most stable GS arrangement for this adduct (+0.7 kJ mol^{-1} from the calculations). Whereas this experimental observation is consistent with the computational prediction, the very large chemical shift separation of the signals renders the ^{19}F NMR spectra not suitable for a good line shape simulation, especially in the case of the small signals.[22]

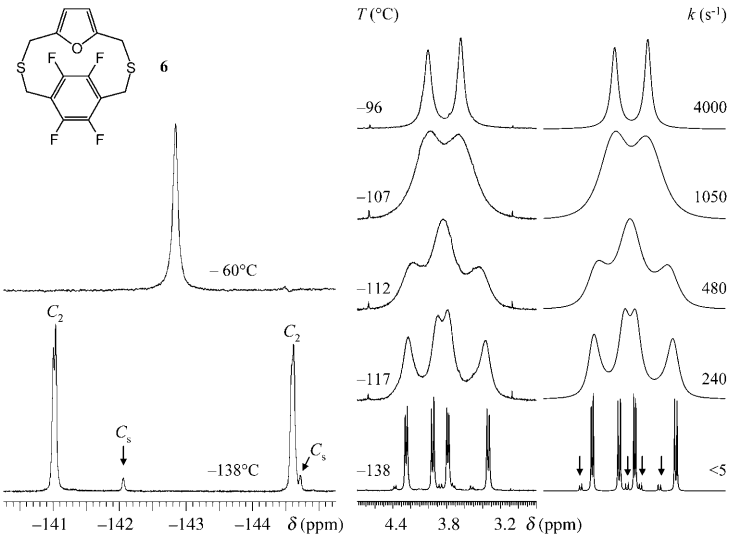

Figure 10. VT-NMR spectra of adduct **6** in $CDFCl_2/CBrF_3$ 2:1 v/v. Left: ^{19}F NMR spectra (564.6 MHz). Right: ^{1}H NMR (600 MHz) spectra with line shape simulations and rate constants. The arrows indicate the minor conformation with C_s symmetry

The stereodynamic process was better analyzed by monitoring the CH_2 signals in the 600 MHz ^{1}H NMR spectra (Figure 10, right). Each of the two CH_2 singlets observed at RT broadened below −80 °C, coalesced around −110 °C, and eventually split below −115 °C. At −138 °C, two sets of signals, each one comprising two AB systems, were visible with a 94:6 intensity ratio (therefore, four doublets in each set were observed). The presence of only two AB systems in each set of signals indicates that both conformations maintain a symmetry element that relates the two pairs of constitutionally equivalent methylenes (an asymmetric C_1 conformation would show four AB systems, as in the case of compounds **3** and **4**). In agreement with the results of the ^{19}F NMR spectroscopic analysis, the major signals were assigned to the C_2-symmetric conformation GS-4 and the minor ones to the C_s-symmetric conformation GS-3. The simulation of the spectra at various temperatures showed that the line shape analysis could be performed by using a single set of rate constants.[23] This observation implies that the process that exchanges the pairs of enantiomeric C_2 conformers (a racemization process) is the same that generates the C_s-symmetric conformation.

This is in agreement with the analysis based on DFT calculations, which predicted that the threshold mechanism for the interconversion of the enantiomeric C_2 conformations (racemization) must leap over TS-1. The experimental value of +30.1 kJ mol^{-1} obtained by the line shape simulation of the proton spectra nicely agrees with the calculated energy barrier of +33.0 kJ mol^{-1}. Following the theoretical analysis, the GS-2 (C_1) and the TS-2 conformations were visited during the racemization process. However, this part of the stereodynamic pathway is invisible to NMR spectroscopy because GS-2 is too high in energy to be populated (calcd value: +18.0 kJ mol^{-1}), and TS-2 is too low in energy with respect to the threshold mechanism TS-1. The corresponding process could be observable only if the GS-2 conformation were populated.

In the case of the nonfluorinated cyclophane **5**, the calculations predicted the GS-3 C_s-symmetric structure to be slightly more stable than the GS-4 C_2 conformation. However, VT-^{1}H NMR spectroscopic analysis of the aromatic region of the spectrum of adduct **5** (in $CDFCl_2/CBrF_3$) experimentally indicated a different conformational preference for this compound (Figure 11).

Indeed, the singlet observed for the benzene protons at room temperature broadened on lowering the temperature and split below −125 °C. The presence of coupled phenyl protons in the spectrum recorded at −150 °C showed that, as in the case of adduct **6**, the more populated conformation

 © 2010 Wiley-VCH Verlag GmbH & Co. KGaA, Weinheim

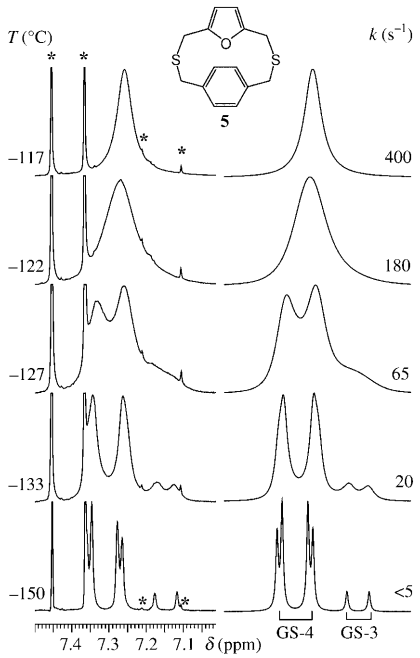

Figure 11. Left: ^{1}H NMR spectra of the aromatic region of adduct **5** (600 MHz in $CDFCl_2/CBrF_3$). The stars indicate the residual proton signals of the solvents. Right: line shape simulation with the corresponding rate constants.

was the C_2-symmetric GS-4, in which the diastereotopic *ortho* phenyl hydrogen atoms belonging to the same side of the benzene ring are coupled with $^3J(H,H) = 7.5$ Hz. In the case of cyclophane **5**, the C_s-symmetric minor conformation GS-3 was experimentally found to be more populated than the corresponding conformation of adduct **6**, the GS-4/GS-3 population ratio being 88:12 at −150 °C. This ratio corresponds to $\Delta G° = +2.0$ kJ mol^{-1} between GS-4 and GS-3. As in the case of **6**, a satisfactory line shape simulation could be carried out by using a single rate constant. By this analysis, an experimental energy barrier of 29.7 kJ mol^{-1} was determined for the threshold process that exchanges the enantiomers of conformation GS-4 and interconverts GS-4 with GS-3. This value nicely agrees with that calculated by DFT (31.8 kJ mol^{-1}). As in the case of **6**, the barrier corresponding to the lower energy TS-2 could not be determined experimentally.

Therefore, the results of the NMR spectroscopic analysis showed that in the case of adduct **5**, the DFT calculations failed to correctly predict the ground-state geometry. To try and explain this observation, it has to be taken into account that the C_2 conformation is favored by the entropy of mixing, since the GS-4 conformation of C_2 symmetry comprises two enantiomers, whereas the C_s-symmetric conformation GS-3 does not.[24] Accordingly, the computed energy of the C_2 conformation GS-4 of **5** has to be lowered by an entropic factor of $RT \times \ln 2 = 1.7$ kJ mol^{-1} with respect to the GS-3 When this effect is considered, the GS-4 conformation is expected to be the most stable conformation (in fact ΔG^0 is 1.5–1.7 = −0.2 kJ mol^{-1}).[25] It must also be noted that, when B3LYP calculations were performed in the presence of dichloromethane as the solvent (chosen to mimic the difficult-to-parametrize freon mixture actually employed in the NMR spectroscopic experiments) and using the Polarizable Continuum Model with the 6-311++G(2d,p) basis set,[26] the GS-3 conformer was still calculated to be the most stable, even if the computed energy difference was reduced to a negligible value (0.1 kJ mol^{-1}). Calculations with a different and more sophisticated theoretical approach (CISD/6-31 g(d)//B3LYP/6-311++G(2d,p)) also predicted that GS-3 should be more stable than GS-4 by 0.35 kJ mol^{-1}. Thus, all of the calculations concurred to predict GS-3 as the most stable conformation for adduct **5**, even if the energy difference with the experimentally observed minimum GS-4 was very small.

However, the experimental observation could be rationalized by dipolar-moment considerations. The dipole moment calculated in the gas phase for the C_s structure GS-3 is 1.48 D, whereas it corresponds to 0.3 D in the C_2 GS-4 conformer. This difference suggests that the GS-4 conformation should be favored (and observed as the major conformation) in low-polarity solvents, such as the freons used for VT-NMR spectroscopic experiments, and disfavored in a more polar environment.

Discussion

The proposal of a general rationalization encompassing the findings of this and our previous work[10] on structurally related pyridine-derived cyclophanes seems very ambitious. As mentioned above, the geometric differences between hexa-atomic pyridine and penta-atomic thiophene and furan are likely to play a role in determining peculiar conformational preferences for adducts **1**–**6**. This difference would prevent a quantitative comparison of the energetics of the arene/heteroarene interactions, and allow only a qualitative comparison of the stereodynamic behaviors of the cyclophanes across the whole series. On the other hand, a rationalization can be more safely attempted by comparing pairs of compounds that can be considered homogeneous either because they feature the same heterocyclic component and different benzene platforms (such as **3** vs. **4** and **5** vs. **6**), or different heterocycles and the same type of benzene residue (such as **3** vs. **5** and **4** vs. **6**).

Thiophene-containing adducts **3** and **4** have geometrically very similar calculated GS and TS conformations. The most striking difference between these conformations resides in the energy of the threshold TS-2, which is +9.2 (by computation) or +10.0 kJ mol^{-1} (by experiment) higher for adduct **4**, featuring a fluorinated benzene platform, than for H-substituted adduct **3**. Remarkably, for the same pair of adducts, virtually isoenergetic low-energy TS-1 is observed, with an experimentally determined difference of less than 1 kJ mol^{-1}. An explanation for this observation could be found in the fact that overcoming TS-1 does require only the isomerization of one of the two CH_2SCH_2 bridges from

 © 2010 Wiley-VCH Verlag GmbH & Co. KGaA, Weinheim

a *cis* to a *trans* orientation with respect to the other bridge, a minimal conformational movement that does not involve the interacting arenes and, therefore, should not depend on the different substitution pattern at the benzene nucleus of **3** and **4**. On the contrary, passing from the PS conformation corresponding to GS-1 to the EtF arrangement of TS-2 exerts a major effect on the heteroarene/arene interaction and this conformational change is expected to be sensitive to benzene substitution. Thus, with this established, the question as to why the barrier to the latter process is $10\,kJ\,mol^{-1}$ higher for the fluorinated adduct **4** than for **3** must be addressed.

To answer this question, two distinct scenarios must be contemplated. One calls for isoenergetic GSs and TSs of different energy; the other, for GSs of different stability from which TSs of equal energy are reached through similar pathways experiencing analogous steric strain. We believe that the virtually identical distortions that both adducts are undergoing to achieve the thiophene ring-flip mechanism suggests that the second option is the correct one. This hypothesis finds a strong theoretical basis in the calculations (that predict identical conformational movements and structurally related intermediates along the topomerization pathway for **3** and **4**), and experimental support in the observation that very similar barriers have to be overcome to reach TS-1, an isomerization that does not involve a change of the relative orientation of the aromatic systems (see above). The choice of the second scenario leaves us with the necessity of explaining why GS-1 should be more stable in the case of adduct **4** than in the case of **3**. This can be explained on the basis of the interpretation of the interactions between PS arenes that we have previously used for other model systems.[9] Within this framework, the interaction between PS arranged π systems has a strong repulsive component due to the presence of two six-electron π clouds at a close distance. This repulsion can be decreased by subtracting electron density from one[9b] or, even better, from both the arenes.[9c] A very efficient way of achieving this result is represented by extensive introduction on one of the rings of strongly electronegative fluorine atoms.[9d] On this basis, the GS-1 PS conformation of fluorinated cyclophane **4** should be more stable (or less unstable) than that of its analogue **3**, and the difference in the barrier to be overcome to reach the threshold TS should essentially reflect the energetic difference of the GS.

Support for this hypothesis was found when calculations showed different HOMOs for the GS-1 conformation of compound **4** when compared with that of **3**, which indicates a repulsive interaction (Figure 12) between the two electronic clouds of thiophene and benzene, which is greatly reduced in the case of compound **4**.

To conclude this discussion, it must be mentioned that the rationalization based on the minor stability of the orthogonal EtF disposition of TS-2 for adduct **4** than for adduct **3** does not seem plausible. Indeed, it is difficult to rationalize why an arrangement in which the lone pairs of the sulfur atom point toward the centroid of the benzene ring should

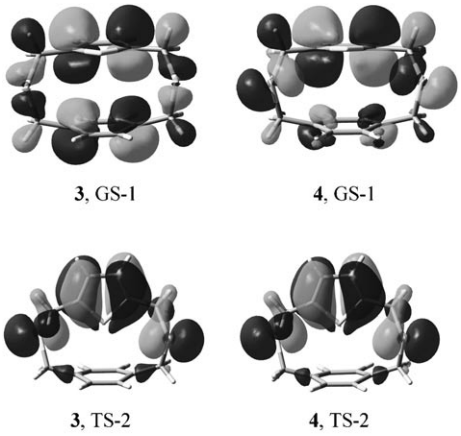

Figure 12. Calculated HOMOs for GS-1 and TS-2 of compounds **3** and **4**. A color version of this figure is available in the Supporting Information.

be less stable in the case of adduct **4** for which, due to the presence of the fluorine atoms, on the benzene centroid there should be less electron density than in the case of **3**. Possibly, because of the short distance between the sulfur atom and the benzene platform (2.85 and 2.84 Å, for **3** and **4**, respectively) and the large size of sulfur (atomic radius 1.09 Å), these EtF dispositions are so sterically hindered that electronic factors become negligible, steric repulsion dominates the interaction, and the TSs are equally disfavored. HOMO analysis further supports this hypothesis, in that the two MOs calculated for the TS-2 conformations were almost identical (Figure 12).

Also furan-containing adducts **5** and **6** have geometrically very similar calculated GS and TS conformations. In striking a difference with the thiophene derivatives, however, for both compounds the low-energy GS conformations feature EtF dispositions of the two rings, and PS conformations, such as GS-2, are high-energy minima. This dramatic change in conformational preference observed on passing from thiophene to furan derivatives needs to be at least tentatively rationalized.

A possible explanation can be proposed by considering that furan is notoriously a much more electron-rich heteroaromatic compound than thiophene.[27] On this basis, a PS disposition should experience a stronger repulsion between the benzene and the heterocyclic ring in the case of furan derivatives **5** and **6** than of thiophene-containing compounds **3** and **4**. This repulsive effect could prevent compounds **5** and **6** from adopting a PS disposition and force them to resort to the observed EtF arrangement. In their turn, the EtF dispositions should be less sterically strained and thus more accessible to adducts **5** and **6** than to adducts **3** and **4**, because the former pair features the presence of an oxygen atom smaller than sulfur above the platform benzene ring (atomic radius for O = 0.65; for S = 1.09 Å) and a shorter C–heteroatom bond distance (C-O = 1.368; C-S = 1.712 Å).[28]

It would be interesting to determine whether the different substitution pattern at the benzene platforms influences the relative stability of the low-energy GS conformations of cyclophanes **5** and **6**. In this case, one can intuitively suppose

 © 2010 Wiley-VCH Verlag GmbH & Co. KGaA, Weinheim

that adduct **6** should be more stable than **5** because in the case of **6** the oxygen lone pairs point toward the centroid of an aromatic ring in which a partial positive charge should reside (or, at least, a deficiency of electron density) because of the presence of the fluorine atoms. However, at a variance with what was observed in the case of the thiophene derivatives, a comparison based on the energy barriers required for the isomerization of **5** and **6** (see Figure 9) cannot be used to evaluate the energy difference of the GS conformations, because the isomerization threshold mechanism does not involve a change of the relative arrangements of the aromatic rings but merely the reorientation of the CH_2SCH_2 bridges. Not surprisingly for **5** and **6**, the energy values of the threshold TSs are virtually identical and insensitive to the substitution at the benzene ring. The fact that there is a very large energy difference between low- and high-energy GS conformations for compounds **5** and **6** (that is between GS-3 and GS-4 on one side and GS-1 and GS-2 on the other, Table 2) and that this difference is much larger in the case of the **5**/**6** pair than in that of the **3**/**4** one, seems to support the interpretation that the EtF disposition is the only one available for the furan-derived adducts.

In summarizing this part of the discussion it could be interesting to check whether the data reported here and in the previous work[10] could allow us to draw some general conclusions on the aromatic/heteroaromatic interaction or, at least on the effect exerted on that interaction by perfluorination of the aromatic ring. However, the fact that similar relative arene/heteroarene dispositions (EtF or PS) correspond to GS conformations for a pair of compounds and to TS conformations for another pair (and vice versa) strongly suggests that this exercise can be highly speculative, and that more experimental work must be carried out to have sufficient data to propose a comprehensive rationalization of the factors affecting the aromatic/heteroaromatic interaction.

As mentioned in the Introduction, one of the reasons that led us to undertake this work concerned the possibility of studying the interaction between the lone pair(s) of oxygen and sulfur and aromatic π systems. Very few experimental studies on model systems have appeared in the literature on this topic. Gung and Amicangelo,[29] by using the conformational preferences of adducts **11** (Scheme 2) showed that, independent of the electron-rich or -poor nature of the aryl residue, there is always a favorable interaction between the oxygen atom of the methyloxymethyl group and the Ar π system, estimating the stabilization effect of the oxygen atom/π interaction at −0.8 to −2.8 kJ mol^{-1}. Remarkably, the interaction becomes clearly more favorable when the Ar group is a pentafluorophenyl residue ($\Delta G° \leq -5.0$ kJ mol^{-1}).

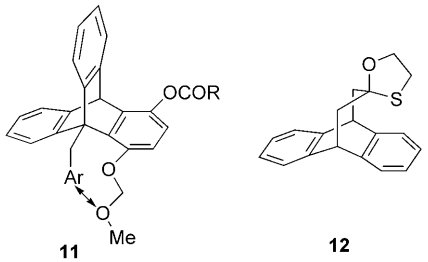

Scheme 2. Structures of model systems **11** and **12**.

In a second study, Motherwell and Aliev[30] showed that adduct **12** preferentially exists in the conformation depicted, featuring a sulfur/π rather than an oxygen atom/π interaction ($\Delta G° = 2.9$ kJ mol^{-1}), and suggested that sulfur's higher polarizability and availability of 3d orbitals can concur to explain this observation.[31] Unfortunately, in our models systems **3** and **4** the only conformation showing exclusively an S/π interaction is the EtF-arranged, high-energy TS-2 (Table 1). The short distance between the heteroatom and the centroid of the platform benzene rings calculated for these conformations (2.85 for **3**; 2.84 Å for **4**) and the large size of the sulfur atom strongly suggests the sterically and electronically repulsive nature of this interaction, on the nature of which any further speculation seems unwarranted. On the other hand, in the case of furan-containing adducts **5** and **6** the O/π interaction occurs in the GS and can be considered as contributing to the stability of the EtF geometry. Even if we have not been able to show whether this stabilization is stronger or weaker depending on the electron-poor or -rich nature of the benzene platform (see above), we believe that the mere existence of these EtF adducts as global minima can be taken as an indication that the O/π interaction can indeed be a favorable one as suggested first by Gung and Amicangelo,[28] and more recently by Swager and Houk.[6c]

In this context, the determination of the X-ray structure of adduct **6** is particularly relevant and deserves a comment on its own. The first theoretical hypothesis about the possible existence of a favorable interaction between an electron-donor atom and hexafluorobenzene dates back to the late 1990s.[32] Notwithstanding intensive theoretical and experimental work,[8] X-ray evidence demonstrating the possible existence of an intramolecular interaction between an ether-type oxygen atom and a pentafluophenyl ring has been reported only once for adduct **11** in Scheme 2, for which Ar = C_6F_5 and R = 4-iodophenyl.[29,31,33]

However, as the authors pointed out, this structural determination suffered from "poor mean bond distances". In addition, the separation between the oxygen atom and the center of the pentafluorophenyl residue was much longer (3.48 Å) than that calculated to be the best for observing the interaction (3.0 Å).[28] The much shorter distance observed in the case of adduct **6** (2.90 Å) can be taken as an indication of a strong interaction probably enforced by the structural constraints of our model systems.

Conclusion

Four simple model systems based on the [3.3]meta(heterocyclo)paracyclophane skeleton were designed and synthesized to study the intramolecular interaction between standard

 © 2010 Wiley-VCH Verlag GmbH & Co. KGaA, Weinheim

heteroaromatic rings and tetra-H- or tetra-F-substituted benzenes. In particular, thiophene- and furan-containing cyclophanes were prepared by high-dilution cyclizations, and a complete conformational analysis was carried out by a combination of calculations and VT-NMR spectroscopic techniques. In general, the predictions of the calculations were nicely confirmed by the NMR spectroscopic experiments. These adducts underwent different types of isomerizations. The conformational preferences of the compounds and the stereodynamic pathways of the isomerization depended on the nature of the heterocycle.

In their ground-state conformation, the thiophene-derived adducts adopted a parallel stacked arrangement of the aromatic systems. The isomerization involved a thiophene ring-flip process passing through an edge-to-face arranged transition state, overcoming a threshold energy barrier that was higher by 10 kJ mol^{-1} in the case of the adduct featuring the perfluorinated benzene ring. This difference was rationalized by assuming that the ground-state conformation of the H-substituted adduct was less stable than that of its fluorinated counterpart because of a stronger repulsion between the electrons of the π systems.

On the contrary, in their ground-state conformations the furan-derived adducts were predicted to adopt an edge-to-face disposition of the rings with the oxygen atom pointing toward the benzene platform. The prediction was confirmed by NMR spectroscopic analysis and by X-ray crystallography. In the case of these adducts, the isomerization process involved distortion of the CH_2SCH_2 bridges and the adoption of transition-state geometries in which the rings were arranged in a parallel-stacked orientation. Once again, a very nice agreement was observed between the predicted and the experimentally determined geometries and pathways. In this case, the threshold barriers were much lower in energy and virtually independent of the presence of fluorine atoms on the platform benzene ring.

We believe that this work, along with our previously reported study on similar [3.3]meta(pyridino)paracyclophanes,[10] can contribute towards the investigation of the two types of interactions, (namely, aromatic/heteroaromatic and lone pair/aromatic interactions), which have been only marginally investigated so far. Even if a comprehensive rationalization of the behavior of the whole series of compounds could not be proposed, mainly because of their different geometric properties, several suggestions emerged from these data. These suggestions can be used as blueprints in designing molecules capable of molecular recognition and in assembling new supramolecular architectures. They can also serve as interpreting tools for explaining nonbonded interactions involving aromatic and heteroaromatic compounds in chemistry and biochemistry.

Experimental Section

Materials: All commercially available reagents including dry solvents were used as received. Organic extracts were dried over sodium sulfate, filtered, and concentrated under vacuum by using a rotary evaporator. Nonvolatile materials were dried under high vacuum. Reactions were monitored by thin-layer chromatography on pre-coated Merck silica gel 60 F254 plates and visualized either by UV or by staining with a solution of cerium sulfate (1 g) and ammonium heptamolybdate tetrahydrate (27 g) in a mixture of water (469 mL) and concentrated sulfuric acid (31 mL). Flash chromatography was performed on Fluka silica gel 60. The RT-NMR spectra were obtained at 500 MHz for ^{1}H-, 125.6 MHz for ^{13}C-, and 470.5 MHz for ^{19}F NMR spectra on a Bruker Avance 500 spectrometer, or at 600 MHz for ^{1}H-, 150.8 MHz for ^{13}C-, and 564.6 MHz for ^{19}F NMR spectra on a Varian INOVA 600 spectrometer.

2,5-Bisbromomethylthiophene (**7**),[11] 2,5-bisbromomethylfuran (**8**),[12] 2,5-bismercaptomethylthiophene (**9**),[7b,13] 2,5-bismercaptomethylfuran (**10**),[7b,13] and 1,4-bisbromomethyl-2,3,5,6-tetrafluoro-benzene[14] were prepared as described. Bisbromides **7** and **8** proved rather unstable (as described in the literature); their purity was checked by ^{1}H NMR spectroscopy and they were used immediately thereafter. Also bisthiols **9** and **10** were used as crude products after purity determination by ^{1}H NMR spectroscopy.

Synthesis of adducts 3–6: These compounds were prepared by following a procedure described for related thiophene-containing cyclophanes.[7c]

3,7-Dithia-1(2,5)thiopheno-5(1,4)benzenacyclooctaphane (3): A solution of commercially available 1,4-bismercaptomethylbenzene (0.34 g, 2 mmol) and of freshly prepared 2,5-bisbromomethylthiophene (**7**) (0.54 g, 2 mmol) in benzene (100 mL) was slowly added (10 h) to a gently refluxing solution of KOH (0.45 g, 8 mmol) and $NaBH_4$ (0.038 g, 1 mmol) in EtOH (600 mL) with mechanical stirring. Stirring was continued overnight. The solvent was evaporated under vacuum and the pale-yellow residue was dissolved in water (50 mL). The aqueous phase was extracted with CH_2Cl_2 (3×15 mL) and the combined organic phases were dried and concentrated to afford the crude product. This was purified by flash chromatography with 90:10 hexanes/ethyl acetate as the eluant to afford the product as a white solid (0.100 g, 18% yield; m.p. of 199–203 °C). The ^{1}H NMR spectrum of the product thus obtained showed the presence of some impurities. Final purification was achieved by preparative HPLC on a Luna C18 column (250×21.2 mm, 10 μm, eluent = acetonitrile/H_2O 90:10 v/v, t_r = 6.10 min). ^{1}H NMR (600 MHz, $CDCl_3$): δ = 6.88 (4H, br s), 6.48 (2H, s), 3.98 (4H, s), 3.85 ppm (4H, s); ^{13}C NMR (150.8 MHz, $CDCl_3$): δ = 143.5, 137.2, 129.1, 124.4, 38.9, 33.3 ppm; elemental analysis calcd (%) for $C_{14}H_{14}S_3$: C 60.39, H 5.07; found: C 60.25, H 5.01.

3,7-Dithia-1(2,5)thiopheno-5(1,4)tetrafluorobenzenacyclooctaphane (4): A solution of freshly prepared 2,5-bismercaptomethylthiophene (**9**) (0.352 g, 2 mmol) and 1,4-bisbromomethyl-2,3,5,6-tetrafluorobenzene (0.672 g, 2 mmol) in benzene (100 mL) was slowly added (10 h) to a gently refluxing solution of KOH (0.45 g, 8 mmol) and $NaBH_4$ (0.038 g, 1 mmol) in EtOH (600 mL) with mechanical stirring. Stirring was continued overnight. The solvent was evaporated under vacuum and the pale-yellow residue was dissolved in water (50 mL). The aqueous phase was extracted with CH_2Cl_2 (3×15 mL) and the combined organic phases were dried and concentrated to afford the crude product. This was purified by flash chromatography with 93:7 hexanes/ethyl acetate as the eluant to afford the product as a white solid (0.154 g, 22% yield; m.p. 170–173 °C). Final purification was achieved by preparative HPLC on a Luna C18 column (250×21.2 mm, 10 μm, eluent = acetonitrile/H_2O 80:20 v/v, t_r = 9.28 min). ^{1}H NMR (600 MHz, $CDCl_3$): δ = 6.69 (2H, s), 4.07 (4H, br s), 3.89 ppm (4H, br s); ^{13}C NMR (150.8 MHz $CDCl_3$): δ = 143.9 (v. br), 142.4, 125.8, 117.4 (m), 33.8, 24.9 ppm; ^{19}F NMR (564.6 MHz, $CDCl_3$): δ = −143.3 ppm; elemental analysis calcd (%) for $C_{14}H_{10}F_4S_3$: C 47.99, H 2.87; found: C 50.15, H, 2.99.

3,7-Dithia-1(2,5)furano-5(1,4)benzenacyclooctaphane (5): A solution of freshly prepared 2,5-bismercaptomethylfuran (**10**) (0.32 g, 2 mmol) and 1,4-bisbromomethylbenzene (0.528 g, 2 mmol) in benzene (100 mL) was slowly added (10 h) to a gently refluxing solution of KOH (0.45 g, 8 mmol) and $NaBH_4$ (0.038 g, 1 mmol) in EtOH (600 mL) with mechanical stirring. Stirring was continued overnight. The solvent was evaporated under vacuum and the pale-yellow residue was dissolved in water (50 mL). The aqueous phase was extracted with CH_2Cl_2 (3×15 mL) and the combined organic phases were dried and concentrated to afford the

 © 2010 Wiley-VCH Verlag GmbH & Co. KGaA, Weinheim

crude product. This was purified by flash chromatography with 90:10 hexanes/ethyl acetate as the eluant to afford the product as a white solid (0.105 g, 20% yield; m.p. 133–136°C). Final purification was achieved by preparative HPLC on a Luna C18 column (250×21.2 mm, 10 μm, eluent = acetonitrile/H_2O 90:10 v/v, t_r = 5.56 min). ^{1}H NMR (500 MHz, $CDCl_3$): δ = 7.15 (4H, s), 5.82 (2H, s), 3.88 (4H, s), 3.44 ppm (4H, s); ^{13}C NMR (125.6 MHz, $CDCl_3$): δ = 152.5, 136.2, 129.4, 107.7, 38.0, 26.8 ppm; elemental analysis calcd (%) for $C_{14}H_{14}OS_2$: C 64.09, H 5.38; found: C 63.96, H 5.44.

3,7-Dithia-1(2,5)furano-5(1,4)tetrafluorobenzenacyclooctaphane (6): A solution of freshly prepared 2,5-bismercaptomethylfuran (**10**) (0.32 g, 2 mmol) and 1,4-bisbromomethyl-2,3,5,6-tetra-fluorobenzene (0.672 g, 2 mmol) in benzene (100 mL) was slowly added (10 h) to a gently refluxing solution of KOH (0.45 g, 8 mmol) and $NaBH_4$ (0.038 g, 1 mmol) in EtOH (600 mL) with mechanical stirring. Stirring was continued overnight. The solvent was evaporated under vacuum and the pale-yellow residue was dissolved in water (50 mL). The aqueous phase was extracted with CH_2Cl_2 (3×15 mL) and the combined organic phases were dried and concentrated to afford the crude product. This was purified by flash chromatography with 90:10 hexanes/ethyl acetate as the eluant to afford the product as a white solid. The ^{1}H NMR spectrum showed some impurities that were removed by crystallization from acetonitrile to afford the product (0.067 g, 10% yield; m.p. 176–177°C). ^{1}H NMR (500 MHz, $CDCl_3$): δ = 5.95 (2H, s), 3.97 (4H, s), 3.60 ppm (4H, s); ^{13}C NMR (125.6 MHz, $CDCl_3$): δ = 152.1, 145.0 (dd, J = 248, 11), 116.3, 108.8, 27.6, 24.6 ppm; ^{19}F NMR (470.5 MHz, $CDCl_3$): δ = −144.0 ppm; elemental analysis calcd (%) for $C_{14}H_{10}F_4S_3$: C 50.29, H 3.01; found: C 50.17, H 3.07; crystals suitable for X-ray analysis were obtained by slow evaporation of an acetonitrile solution: $C_{14}H_{10}F_4OS_2$ (M_r = 334.34); data recorded at 298°C with $Mo_{K\alpha}$ radiation (0.71073 Å); crystal dimensions 0.3×0.2×0.2 mm; μ = 0.441 mm^{-1}; monoclinic; space group $P2_1/c$; a = 12.5420(16), b = 12.5640(16), c = 8.9097(11) Å; β = 108.1730(10); V = 1333.9 Å^3; Z = 4; $-16 \le h \le 16$, $-16 \le k \le 16$, $-12 \le l \le 11$; 15142 reflections ($1.71° < 2\theta < 28.69°$); 3260 independent reflections; R = 0.033 for 2926 data [$I > 2\sigma(I)$]; wR = 0.0935; CCDC-769240 contains the supplementary crystallographic data for this paper. These data can be obtained free of charge from The Cambridge Crystallographic Data Centre via www.ccdc.cam.ac.uk/data_request/cif.

VT-NMR spectroscopy:[34] The VT-NMR spectra were recorded at 600 MHz for ^{1}H-, 150.8 MHz for ^{13}C-, and 564.6 MHz for ^{19}F NMR spectra, by using a broadband variable-temperature customized probe from Z-Spec. Where required, the assignments of the ^{1}H and ^{13}C signals were obtained by bi-dimensional experiments (edited-gsHSQC[35] and gsHMBC[36]). The samples for obtaining spectra at temperatures lower than −100°C were prepared by connecting the NMR tubes containing the compound to a vacuum line and condensing therein the gaseous Freons (CHF_2Cl, $CDFCl_2$,[37] and $CBrF_3$ or mixtures of them) with cooling by liquid nitrogen. The tubes were subsequently sealed under vacuum and introduced into the cooled probe of the spectrometer. Temperature calibrations were performed before the experiments, by using a Cu/Ni thermocouple immersed in a dummy sample tube filled with isopentane, and under conditions as nearly identical as possible. The uncertainty in the temperatures was estimated from the calibration curve to be ±2°C. The line shape simulations were performed by means of a PC version of the QCPE program DNMR6 n° 633, Indiana University, Bloomington, IN.

Calculations: Conformational searches were performed by Moleculam Mecahnics (MMFF force Field as implemented in Titan 1.0.5, Wavefunction inc.). Final geometry optimizations were carried out at the B3LYP/6–311++G(2d,p) level by means of the Gaussian 03 series of programs.[16] In the case of **6**, geometry optimizations were also carried out including the solvent (dichloromethane) by using the PCM approach.[26] The standard Berny algorithm in redundant internal coordinates and default criteria of convergence were employed in all the calculations. Harmonic vibrational frequencies were calculated for all the stationary points. For each optimized ground state the frequency analysis showed the absence of imaginary frequencies, whereas each transition state showed a single imaginary frequency. Visual inspection of the corresponding normal mode was used to confirm that the right transition state had been found.[38] All the reported energy values represent total electronic energies. In general, these give the best fit with experimental DNMR spectral data.[39] Therefore, the computed numbers have not been corrected for zero-point energy contributions or other thermodynamic parameters. This avoids artifacts that might result from the inevitably ambiguous choice of an adequate reference temperature, from empirical scaling tuned for a better matching of experimental and theoretical numbers[40] and from the treatment of low-frequency vibration as harmonic oscillators. This is particularly important in the present case, for which many calculated frequencies fall below the 500–600 cm^{-1} range.[41]

Acknowledgements

Dr. M. Garavelli, University of Bologna, is gratefully acknowledged for helpful comments. A.M. received financial support from the University of Bologna (RFO) and from MUR-COFIN 2007, Rome (PRIN National Project "Stereoselection in Organic Synthesis"). F.C. received financial support from the University of Milano.

[1] Reviews: a) E. A. Meyer, R. K. Castellano, F. Diederich, *Angew. Chem.* **2003**, *115*, 1244–1287; *Angew. Chem. Int. Ed.* **2003**, *42*, 1210–1250; b) S. L. Cockroft, J. Perkins, C. Zonta, H. Adams, S. E. Spey, C. M. R. Low, J. G. Vinter, K. R. Lawson, C. J. Urch, C. A. Hunter, *Org. Biomol. Chem.* **2007**, *5*, 1062–1080.

[2] Review: D. B. Amabilino, J. F. Stoddart, *Chem. Rev.* **1995**, *95*, 2725–2829.

[3] Reviews: a) K. Reichenbächer, H. I. Süss, J. Hulliger, *Chem. Soc. Rev.* **2005**, *34*, 22–30; b) J. D. Dunitz, A. Gavezzotti, *Angew. Chem.* **2005**, *117*, 1796–1819; *Angew. Chem. Int. Ed.* **2005**, *44*, 1766–1787.

[4] Review: M. L. Waters, *Curr. Opin. Chem. Biol.* **2002**, *6*, 736–741.

[5] a) P. A. Williams, J. Cosme, A. Ward, H. C. Angove, D. M. Vinkovic, H. Jhoti, *Nature* **2003**, *424*, 464–468; b) S. Vandenbussche, D. Diaz, M. C. Fernandez-Alonso, W. Pan, S. P. Vincent, G. Cuevas, F. J. Cañada, J. Jiménez-Barbero, K. Bartik, *Chem. Eur. J.* **2008**, *14*, 7570–7578; c) Z. R. Laughrey, S. E. Kiehna, A. J. Riemen, M. L. Waters, *J. Am. Chem. Soc.* **2008**, *130*, 14625–14633; d) P.-L. Zhao, L. Wang, X.-L. Zhu, X. Huang, C.-G. Zhan, J.-W. Wu, G.-F. Yang, *J. Am. Chem. Soc.* **2010**, *132*, 1185–1194.

[6] Reviews: a) C. A. Hunter, K. R. Lawson, J. Perkins, C. J. Urch, *J. Chem. Soc. Perkin Trans. 2* **2001**, 651–669; b) W. B. Jennings, B. M. Farrell, J. F. Malone, *Theor. Chem. Acc.* **2001**, *34*, 885–894; a recent themed issue of the journal *Phys. Chem. Chem. Phys.* was devoted to studies on arene–arene interactions: *Phys. Chem. Chem. Phys.* **2008**, *10*(19), 2581–2868; c) for a very recent article presenting a comprehensive and critic discussion of the most popular rationalization of the arene–arene interactions, see: S. E. Wheeler, A. J. McNeil, P. Mueller, T. M. Swager, K. N. Houk, *J. Am. Chem. Soc.* **2010**, *132*, 3304–3311.

[7] a) Y. Fukazawa, J. Tsuchiya, M. Sobukawa, S. Itô, *Tetrahedron Lett.* **1985**, *26*, 5473–5476; b) Y. Fukazawa, M. Kodama, J. Tsuchiya, Y. Fugise, S. Itô, *Tetrahedron Lett.* **1986**, *27*, 1929–1932; c) M. Takeshita, M. Tashiro, A. Tsuge, *Chem. Ber.* **1991**, *124*, 1403–1409; d) A. Bahl, W. Grahn, S. Stadler, F. Feiner, G. Bourhill, C. Bräuchle, A. Reisner, P. G. Jones, *Angew. Chem.* **1995**, *107*, 1587–1590; *Angew. Chem. Int. Ed. Engl.* **1995**, *34*, 1485–1488; e) J. A. Zoltewicz, N. M. Maier, W. M. F. Fabian, *J. Org. Chem.* **1997**, *62*, 3215–3219, and references therein; f) S. Tsuzuki, K. Honda, R. Azumi, *J. Am. Chem. Soc.* **2002**, *124*, 12200–12209; g) G. E. Tumambac, C. Wolf, *J. Org. Chem.* **2004**, *69*, 2048–2055; h) A. Fürstner, M. Alcarazo, H. Krause, C. W. Lehmann, *J. Am. Chem. Soc.* **2007**, *129*, 12676–12677; i) I. Richter, J. Minari, P. Axe, J. P. Low, T. D. James, K. Sakurai, S. D. Bull, J. S. Fossey, *Chem. Commun.* **2008**, 1082–1084.

[8] Reviews: a) M. Egli, S. Sarkhel, *Acc. Chem. Res.* **2007**, *40*, 197–205; b) B. L. Schottel, H. T. Chifotides, K. R. Dunbar, *Chem. Soc. Rev.*

 © 2010 Wiley-VCH Verlag GmbH & Co. KGaA, Weinheim

2008, *37*, 68–83; c) B. P. Hay, V. S. Bryantsev, *Chem. Commun.* **2008**, 2417–2428; d) O. B. Berryman, D. W. Johnson, *Chem. Commun.* **2009**, 3143–3153.

[9] Review: a) F. Cozzi, J. S. Siegel, *Pure Appl. Chem.* **1995**, *67*, 683–689; b) F. Cozzi, R. Annunziata, M. Cinquini, T. Dwyer, J. S. Siegel, *J. Am. Chem. Soc.* **1992**, *114*, 5729–5733; c) F. Cozzi, R. Annunziata, M. Cinquini, J. S. Siegel, *J. Am. Chem. Soc.* **1993**, *115*, 5330–5331; d) F. Cozzi, M. Cinquini, R. Annunziata, F. Ponzini, J. S. Siegel, *Angew. Chem.* **1995**, *107*, 1092–1094; *Angew. Chem. Int. Ed. Engl.* **1995**, *34*, 1019–1020; e) F. Cozzi, R. Annunziata, M. Benaglia, M. Cinquini, L. Raimondi, K. K. Baldridge, J. S. Siegel, *Org. Biomol. Chem.* **2003**, *1*, 157–162; f) F. Cozzi, R. Annunziata, M. Benaglia, K. K. Baldridge, G. Aguirre, J. Estrada, Y. Sritana-Anant, J. S. Siegel, *Phys. Chem. Chem. Phys.* **2008**, *10*, 2686–2694.

[10] R. Annunziata, M. Benaglia, F. Cozzi, A. Mazzanti, *Chem. Eur. J.* **2009**, *15*, 4373–4381.

[11] P. R. Ashton, J. A. Preece, J. F. Stoddart, M. S. Tolley, A. J. P. White, D. J. Williams, *Synthesis* **1995**, 1344–1346.

[12] D. J. Nielsen, K. J. Cavell, M. S. Viciu, S. P. Nolan, B. W. Skelton, A. H. White, *J. Organomet. Chem.* **2005**, *690*, 6133–6142.

[13] a) K. Y. Novitskii, V. P. Volkov, P. V. Kostetskii, Y. K. Yu'rev, *Zhur. Obschhei Khim.* **1960**, *30*, 2203–2207; K. Y. Novitskii, V. P. Volkov, P. V. Kostetskii, Y. K. Yu'rev, *Zhur. Obschhei Khim.* **1961**, *64*, 9405; b) J. Houk, G. M. Whitesides, *J. Am. Chem. Soc.* **1987**, *109*, 6825–6836.

[14] F. C. Krebs, T. Jensen, *J. Fluorine Chem.* **2003**, *120*, 77–84.

[15] F. Vögtle, R. Lichtentäler, *Chem.-Ztg.* **1970**, *94*, 727.

[16] Gaussian 03, Revision E.01, M. J. Frisch, G. W. Trucks, H. B. Schlegel, G. E. Scuseria, M. A. Robb, J. R. Cheeseman, J. A. Montgomery, Jr., T. Vreven, K. N. Kudin, J. C. Burant, J. M. Millam, S. S. Iyengar, J. Tomasi, V. Barone, B. Mennucci, M. Cossi, G. Scalmani, N. Rega, G. A. Petersson, H. Nakatsuji, M. Hada, M. Ehara, K. Toyota, R. Fukuda, J. Hasegawa, M. Ishida, T. Nakajima, Y. Honda, O. Kitao, H. Nakai, M. Klene, X. Li, J. E. Knox, H. P. Hratchian, J. B. Cross, V. Bakken, C. Adamo, J. Jaramillo, R. Gomperts, R. E. Stratmann, O. Yazyev, A. J. Austin, R. Cammi, C. Pomelli, J. W. Ochterski, P. Y. Ayala, K. Morokuma, G. A. Voth, P. Salvador, J. J. Dannenberg, V. G. Zakrzewski, S. Dapprich, A. D. Daniels, M. C. Strain, O. Farkas, D. K. Malick, A. D. Rabuck, K. Raghavachari, J. B. Foresman, J. V. Ortiz, Q. Cui, A. G. Baboul, S. Clifford, J. Cioslowski, B. B. Stefanov, G. Liu, A. Liashenko, P. Piskorz, I. Komaromi, R. L. Martin, D. J. Fox, T. Keith, M. A. Al-Laham, C. Y. Peng, A. Nanayakkara, M. Challacombe, P. M. W. Gill, B. Johnson, W. Chen, M. W. Wong, C. Gonzalez, J. A. Pople, Gaussian Inc., Wallingford CT, **2004**.

[17] The interplanar angle represents the deviation from the situation in which the two rings are parallel to each other.

[18] a) K. Mislow, M. Raban, *Top. Stereochem.* **1967**, *1*, 1–38; b) W. B. Jennings, *Chem. Rev.* **1975**, *75*, 307–322; c) E. L. Eliel, *J. Chem. Educ.* **1980**, *57*, 52; d) D. Casarini, L. Lunazzi, D. Macciantelli, *J. Chem. Soc. Perkin Trans. 2* **1992**, 1363–1370.

[19] In principle, a $^{4}J_{F-F}$ *meta* coupling could be visible, but the lines were too broad and the coupling too small to be observed in this case.

[20] a) W. R. Jackson, *Tetrahedron Lett.* **1974**, *15*, 1837–1838; b) J. E. Anderson, D. Casarini, A. J. Ijeh, L. Lunazzi, *J. Am. Chem. Soc.* **1997**, *119*, 8050–8057; c) D. Casarini, L. Lunazzi, A. Mazzanti, E. Foresti, *J. Org. Chem.* **1998**, *63*, 4746–4754; d) L. Lunazzi, A. Mazzanti, S. Rafi, H. S. P. Rao, *J. Org. Chem.* **2008**, *73*, 678–688.

[21] a) N. Okazawa, T. S. Sorensen, *Can. J. Chem.* **1978**, *56*, 2737–2742; b) F. A. L. Anet, V. J. Basus, *J. Magn. Reson. (1969-1992)* **1978**, *32*, 339–343; c) J. Sandström, *Dynamic NMR Spectroscopy*, Academic Press, London, **1982**, pp. 81–84.

[22] When the exchange took place, the lines became extremely broad and the signal/noise ratio was very low; therefore, the reliability of the simulation greatly decreased.

[23] The simulation must take into account also how the populations change on changing the temperature (Boltzmann rule); in this case, the 94:6 population ratio at −138 °C becomes 92:8, 91:9, and 90:10 at −117, −112 and −107 °C, respectively.

[24] E. L. Eliel, S. H. Wilen in *Stereochemistry of Organic Compounds*, Wiley, New York, **1994**, p. 97 and E. L. Eliel, S. H. Wilen in *Stereochemistry of Organic Compounds*, Wiley, New York, **1994**, p. 601. See also: L. Lunazzi, A. Mazzanti, M. Minzoni, *J. Org. Chem.* **2005**, *70*, 10062–10066.

[25] The entropic correction is temperature-dependent; therefore, at low temperature the ratio can be reversed.

[26] Review: J. Tomasi, B. Mennucci, R. Cammi, *Chem. Rev.* **2005**, *105*, 2999–3093.

[27] G. Marino in *Advances in Heterocyclic Chemistry, Vol. 13* (Eds.: A. R. Katrizky, A. J. Boulton), Academic Press, New York, **197**1, pp. 235–314.

[28] A. G. Orpen, L. Brammer, F. H. Allen, O. Kennard, D. G. Watson, R. Taylor in *Structure Correlations, Vol. 2* (Eds.: H. B. Burgi, J. D. Dunitz), VCH, Weinheim, **1994**, Appendix A. DFT calculations actually show a C−O distance of 1.368 Å and a C-S distance of 1.752 Å.

[29] B. W. Gung, Y. Zou, Z. Xu, J. C. Amicangelo, D. G. Irwin, S. Ma, H.-C. Zhou, *J. Org. Chem.* **2008**, *73*, 689–693.

[30] W. B. Motherwell, J. Moïse, A. E. Aliev, M. Nic, S. J. Coles, P. H. Horton, M. B. Hursthouse, G. Chessari, C. A. Hunter, J. G. Vinter, *Angew. Chem.* **2007**, *119*, 7969–7972; *Angew. Chem. Int. Ed.* **2007**, *46*, 7823–7826.

[31] For an early discussion on sulfur/π interactions, see: R. S. Morgan, C. E. Tatsch, R. H. Gushard, J. M. McAdon, P. K. Warme, *Int. J. Pept. Prot. Res.* **1978**, *11*, 209–217.

[32] a) I. Alkorta, I. Rozas, J. Elguero, *J. Org. Chem.* **1997**, *62*, 4687–4691; b) J. P. Gallivan, D. A. Dougherty, *Org. Lett.* **1999**, *1*, 103–105; c) Y. Danten, T. Tassaing, M. Besnard, *J. Phys. Chem. A* **1999**, *103*, 3530–3534; for a comparison between O/benzene versus O/hexafluorobenzene interactions, see: d) M. Raimondi, G. Calderoni, A. Famulari, L. Raimondi, F. Cozzi, *J. Phys. Chem. A* **2003**, *107*, 772–774.

[33] For recent reports on the intermolecular interaction between a pentafluorophenyl ring and an hydroxyl oxygen atom see: a) T. Korenaga, H. Tanaka, T. Ema, T. Sakai, *J. Fluorine Chem.* **2003**, *122*, 201–205; b) T. Korenaga, T. Shoji, K. Onoue, T. Sakai, *Chem. Commun.* **2009**, 4678–4680.

[34] Review: D. Casarini, L. Lunazzi, A. Mazzanti, *Eur. J. Org. Chem.* **2010**, 2035–2056.

[35] a) S. A. Bradley, K. Krishnamurthy, *Magn. Reson. Chem.* **2005**, *43*, 117–123; b) E. Kupče, R. Freeman, *J. Magn. Reson. Ser. A* **1996**, *118*, 299–303; c) W. Willker, D. Leibfritz, R. Kerssebaum, W. Bermel, *Magn. Reson. Chem.* **1993**, *31*, 287–292.

[36] R. E. Hurd, B. K. John, *J. Magn. Reson. (1969-1992)* **1991**, *91*, 648–653.

[37] Prepared according to: J. S. Siegel, F. A. L. Anet, *J. Org. Chem.* **1988**, *53*, 2629–2630.

[38] Gaussview 4.1.2, Gaussian Inc, Wallingford, CT, **2006**.

[39] P. Y. Ayala, H. B. Schlegel, *J. Chem. Phys.* **1998**, *108*, 2314–2325.

[40] C. F. Tormena, R. Rittner, R. J. Abraham, E. A. Basso, B. C. Fiorin, *J. Phys. Org. Chem.* **2004**, *17*, 42–48.

[41] M. W. Wong, *Chem. Phys. Lett.* **1996**, *256*, 391–399.

Received: March 29, 2010
Published online: June 16, 2010

 © 2010 Wiley-VCH Verlag GmbH & Co. KGaA, Weinheim